

Supporting Information

I.	Materials and Methods	1
II.	Bulk population dynamics with strong bottlenecks	5
III.	Bulk population dynamics in the large population limit	8
	Supporting Figure Captions	10
	Supporting Table Captions	11

I: Materials and Methods

Yeast strains and experimental evolution

Yeast strains KV948 and KV653 were acquired from the Verstrepen lab (Verstrepen et al. 2005; Legendre et al. 2007). These haploid strains are derived from S288C and contain an engineered *URA3* gene with 7.5 and 68 (AC)-repeats insertions, respectively (Fig. S1). For fluctuating selection, we use synthetic complete (SC) plates with 4% glucose, either drop out uracil (SC-ura) or supplemented with 1.0 (g/L) 5-fluoroorotic acid (SC+5FOA) as selective and counter-selective plates, respectively. For neutral evolution, SC plates with 4% glucose were used.

KV653 was first grown on a YPD plate, and 4 colonies were picked as founders of 8 lineages. For these 4 colonies, halves of the colonies were streaked using plastic tips onto counter-selective plates to generate the A1~A4 lineages; the other halves of these colonies were streaked using different plastic tips onto selective plates to generate the B1~B4 lineages. All A- and B- lineages underwent fluctuating selection for 25 alternating passages on selective/counter-selective plates (Figs. 2 & S2). During each passage, a single surviving colony was randomly picked by plastic tip from the previous plate and spread onto the next plate to yield new colonies. When no colony survived in a lineage, another colony was picked from a different lineage to continue after the extinction event. The newly-streaked plate was incubated at 30°C for two days. After streaking, the residual yeast on the plastic tip was used to inoculate an overnight YPD liquid culture as a record of the evolutionary history. The overnight liquid cultures were collected the next day, made into 15% glycerol yeast stock, and stored in -80°C until further analysis.

For neutral evolution, the procedure was similar except in using the SC plates for each of 25 passages (no selection). Eight neutral lineages were passaged, and two lineages were analyzed.

Determination of evolved tandem repeat lengths

For each node of the evolved lineage, the yeast glycerol stocks from -80°C were thawed and a portion of yeast was spread on a YPD plate to generate a 1 cm square yeast lawn. After two days

incubation at 30°C, about a quarter of each yeast lawn was used for genomic DNA preparation. We used the temperature-difference method for genomic DNA extraction. Briefly, yeast collected from the lawn was washed by TE buffer and re-suspended in lysis buffer (Hoffman and Winston 1987). The solution was then heated in 100°C boiling water for 2 min and immediately frozen at -80°C for 5 min. The treatment was repeated twice to ensure lysis of the yeast cell wall. Then, the cell lysate underwent standard phenol-chloroform extraction and ethanol precipitation. The yeast genomic DNA was dissolved in TE buffer at a concentration approximately 500 ng/μl.

Primers flanking the TR region inside the *URA3* gene (Fig. S1A) were used for the PCR reaction. Forward: 5'GGTATATATACGCATATGTGGTGTGAAGA; reverse: 5'ATTCCTTGGTGGTACGAACATCCAATGAAG. The 5' end of the forward primer was conjugated with a FAM dye. All PCR reactions were performed by using Taq polymerase (Invitrogen 18038-018) with an annealing temperature of 54°C and an elongation time of 1.5 min for 32 cycles. An additional 20 min at 72°C after the last cycle allowed a 3'-overhang adenosine to be added to PCR products. PCR products were treated with ExoSAP-IT kit (Affymetrix 78200) to remove small unwanted oligos. For each evolved node, at least 3 PCR replicates were performed.

PCR products in TR regions are known to have highly variable lengths and often yield multiple peaks, consistent with our findings (Fig. S3) (Hite et al. 1996; Shinde et al. 2003; Olejniczak and Krzyzosiak 2006). We attempted to reduce this variability by using different DNA polymerases (including Phusion, AmpliTaq, and ordinary Taq), different template conditions, and different cycle numbers to optimize the protocol. We found no significant improvement using the proofreading enzymes or when reducing the number of cycles.

To determine fragment lengths, we used customized DNA ladders synthesized by BioVentures, Inc. The double-stranded DNA ladders were conjugated with ROX dye and contained either 5 bp or 10 bp differences within a 200 – 380 bp range. The PCR products and DNA ladders were mixed and submitted for DNA fragment analysis by Genewiz, Inc. The fragment analysis results include intensity data vectors of the ROX channel (DNA ladder) and the FAM channel (PCR product). We used a *Matlab* script to align relevant regions of the intensity data vectors. The algorithm shifts one data vector relative to the other to minimize the square difference between two vectors. For each pair of successive nodes, we first aligned their ROX channels which acts as a reference for length measurements. We then performed another alignment between the FAM channels to estimate their relative length difference. For small indels (<10 bp), estimated differences were usually close to integers within 0.1 bp, and we rounded off the value to the nearest integer to determine indel sizes. For large indels (>10 bp) the error was typically ~ 0.5 bp, and rounding introduced uncertainty of ± 1 bp. This uncertainty was resolved using selection/counter-selection information to determine the frame, and validated using subsequent nodes in the trajectory after a large indel.

Mutation rate and survival frequency measurements

Mutation rates were measured by standard fluctuation analysis (Lang and Murray 2008), using the distribution of colony numbers in parallel cultures which were fit to a Luria-Delbruck distribution (Delbruck 1943). The yeast population was first diluted to approximately 500-1000 cells (for KV653 and KV653-derived strains) or 10^6 cells (for KV948) and inoculated into 200 μ l YPD medium in a 96-well plate. 20 to 30 parallel cultures were inoculated and incubated at 30°C for 16 hrs, and then plated on selective plates (SC-ura 2% glucose), or counter-selective plates (SC+5FOA 2% glucose). Additional 3-5 parallel cultures were diluted and plated on non-selective plates (SC medium 2% glucose) for counting the total cell number. Colonies were counted using a colony counter (aCOLyte 3) after 38 to 40 hrs incubation at 30°C. Parameters were set to count only colonies with diameter > 1mm. We used the MSS-maximum-likelihood method (W. T. Ma 1992; Rosche and Foster 2000) to obtain the optimal estimation of the mutant number, m , and converted this into mutation rate by normalizing to the population size. Confidence intervals were determined as in (Rosche and Foster 2000).

Growth rate measurement

Yeast strains were grown overnight in SC liquid culture and then diluted in 25 ml of SC or SC+5FOA liquid medium with initial $OD_{600} \sim 0.02$. Growth curves were obtained by measuring OD every hour for 6 – 8 data points. Growth rates were calculated by fitting the growth curve to exponential growth in the region of $OD_{600} = 0.1 - 0.8$.

Population dynamics simulations of fluctuating selection

Simulations described below are performed using a Gillespie-type algorithm (Gillespie 2007) implemented in C. All reproductive and mutation events are recorded along with the full genealogical relationships within the simulated population. The ancestral lineage is analyzed by choosing randomly a single cell at the end of each simulation. We used two variants of a simple population dynamics:

Variant A (Figs. 4A,B & S5). The environmental state is alternated between selection and counter-selection after each colony passage step. During colony passage, a single population (macrocolony) is partitioned into many microcolonies, consisting of a Poisson-distributed number of cells with mean n . Each microcolony is allowed to grow until reaching size N_{max} (see values in Table 4). Among all colonies that reached macroscopic size of at least 10^4 cells, a single colony is randomly chosen, partitioned, and so forth. If no colonies reached macroscopic size, the simulation terminates with extinction. For each cell, we track the TR length l , which can mutate by indels according to parameters in Table S4. Small indels change the TR length by 2 units. Large insertions are modeled by uniformly choosing a new value between $l+2$ and $2l$ (inclusive); and large deletions by choosing a value between 0 and $l - 2$ (inclusive). Cells are defined to be ON if l is a multiple of 3, and OFF otherwise. If the length becomes zero, the cell's TR remains zero for the duration of the

simulation. Growth rates in three different frames depend on the environmental state (Table S4).

Variation B (Fig. 4C,D). We follow a single population without partitioning into microcolonies, resampling down to N_{min} cells each time the population reaches size N_{max} . Environmental switching occurs independently of resampling, with period τ . We consider a model with two phenotypes and two environments, where the adapted phenotype in each environment grows with rate 1 (which sets the simulation timescale), and the non-adapted phenotype with rate 0. Switching between phenotypes occurs at rate u .

Modeling 2-bps TR oscillation probability

In the main text, we defined the parameter q (see Eq. 1) to be the probability of a single TR oscillation cycle of a 2 bp insertion and 2 bp deletion. Assuming all insertion/deletion events are independent, the number of oscillations follows a geometric distribution with parameter q .

Our goal is to use experimental data to estimate q , as follows. For each lineage, we start from the first counter-selective node and count the number of TR oscillations that happen. If no TR oscillation is observed then the oscillation number is 0. A TR oscillation segment ends when an event other than a 2 bp insertion or deletion occurs. A new TR segment restarts from the next counter-selective node.

The results are summarized in the table below. If a TR oscillation ends by lineage extinction, we mark it E . If the oscillation persists to the end of the evolution experiment, we mark an additional + sign to denote unfinished counting.

Lineage name	# of oscillations in each segment	Lineage name	# of oscillations in each segment
A1	0, 4, E	B1	1, 0, 2, 1, 3 ⁺
A2	0, 4, E	B2	E
A3	1, E	B3	4, 7 ⁺
A4	1, E	B4	1, E
A1a	1, 8 ⁺	B4a	1, 9 ⁺
A1b	1, 4, 2 ⁺	B3a	2, 0, 0, E
A1c	2, 0, 2 ⁺	B1a	1, E
A1d	1, 1, 3 ⁺		

We use the maximum likelihood method to estimate the parameter q , assuming all insertion/deletion events are independent. The probability to have a TR oscillation segment length equal to k is $q^k(1-q)$, and the probability to have length $\geq k$ is q^k , which is used to account for segments that persist to the end of the experiment. The total likelihood of the observed data, or the objective function $L(q)$, is given by

$$L(q) = \prod_{i=1}^{n_F} q^{k_i} (1-q) \times \prod_{j=1}^{n_U} q^{k_j^+},$$

where n_F is the number of segments that ended by mutation or extinction, and n_U is the number of segments that persisted to the end of the experiment. By differentiating $L(q)$ with respect to q , we obtained the maximal likelihood estimate:

$$\hat{q} = \left(\sum_i k_i + \sum_j k_j^+ \right) / \left(n_F + \sum_i k_i + \sum_j k_j^+ \right).$$

The 90% confidence interval is obtained by approximating $u = \log(L(q))$ locally as a normal distribution around the maximum, and using the formula

$$CI(90\%) \approx \hat{q} \pm \frac{1.65}{\sqrt{-u''(\hat{q})}}.$$

In our data, we have $\sum_i k_i = 33$, $\sum_j k_j^+ = 34$, $n_F = 24$, $n_U = 7$, which yields $\hat{q} = 0.736$, with $CI(90\%) = [0.614, 0.858]$.

II: Bulk population dynamics with strong bottlenecks

In this section we present a population dynamics model tailored for the indel-evolution experiment. We focus on calculating a key measure r , the fraction of environmental switches in which the population makes use of ancestral alleles to survive. The ancestral allele mechanism utilizes residual cells from a previous passage that are transferred into the next environment. The derived allele mechanism utilizes novel mutant cells, and depends on mutation rate u , population size N , and the fraction of mutants that survived in the next environment. As a rough estimate, suppose we have n residual cells and m novel mutant cells in a colony before passage; then r can be approximated by

$r = \frac{n}{n+m}$. However, in a stochastic model, both n and m are random variables and we need to

compute $r = \left\langle \frac{n}{n+m} \right\rangle$, where the bracket represents averaging over the probability distribution

obtained from the stochastic model. In the limit of small mutation rates, we obtain φ , defined in the main text using the approximation $\varphi \approx 1 - r$.

To calculate r explicitly, we assume that every time a yeast cell replicates, the daughter cell has probability u to have an indel mutation. We classify mutational outcomes into six types A_0, \dots, A_5 with mutation probabilities as follows:

A_0 : no indel mutation	$a_0 = \Pr\{A_0\} = 1 - u$
A_1 : 2 bp deletion	$a_1 = \Pr\{A_1\} = (1 - J)u / 2$
A_2 : 2 bp insertion	$a_2 = \Pr\{A_2\} = (1 - J)u / 2$
A_3 : all other indel mutations yielding TR length $l \equiv 0(\text{mod } 3)$	$a_3 = \Pr\{A_3\} = Ju/3$
A_4 : all other indel mutations yielding TR length $l \equiv 1(\text{mod } 3)$	$a_4 = \Pr\{A_4\} = Ju/3$
A_5 : all other indel mutations yielding TR length $l \equiv 2(\text{mod } 3)$	$a_5 = \Pr\{A_5\} = Ju/3$

Here, the parameter J is the probability of large indels ($l > 2$ bp). Large indels can ‘land’ in the three different frames with equal probability. J also depends on the culture medium: in experiments, we observe more large indels in ON->OFF passages than in OFF->ON (see Figure 3).

Given our experimental procedure, we wish to determine before colony passage how many cells within the colony are adapted to the next environment. Let X_j be the number of mutants of type A_j in a colony. The random variables X_0, \dots, X_5 sum to the colony size N , and as we will show below, X_0, \dots, X_5 follows a multinomial distribution. To compute these random variables, let the population initiate from a single cell. In the experiment, the number of cell divisions k for a single cell to give rise to a colony is in the range 18 – 20, and the mutation rate u is in the range $10^{-4} - 10^{-5}$ per cell per generation. Therefore, we employ the following approximations:

1. Since in k cell divisions the population size N does not exceed 10^6 cells, double mutants are ignored as they occur with frequency $\sim u^2 N \ll 1$.
2. Final population size of a colony is always close to 2^k cells, since in the experiment we only pick colonies of average size, and do not pick abnormally small colonies (the exact number depends on how many mutants switch to different frames and their time of occurrence.)
3. The mutants that switched from ON->OFF stop dividing in SC-Ura medium, and the mutants that switched from OFF->ON stop dividing in SC+5FOA medium.

Assumption 3, which is biologically reasonable in our experiment, guarantees that the *number of*

mutants is equal to the *number of mutational events*; without this assumption, analysis becomes significantly more difficult as growth and timing of each mutation needs to be accounted for. Given these assumptions, the numbers of each cell type within a colony have a multinomial distribution:

$$\Pr\{X_j = x_j; j = 0, 1, \dots, 5\} = \frac{N!}{\prod_j x_j!} \prod_j a_j^{x_j} \quad [1]$$

Since we assume the colony has $\sim N$ cells, and mutants that switched phenotype are a small fraction ($\sim u$) of the population, the above can be approximated as a Poisson distribution. Let $\lambda_j = Na_j$,

$$\Pr\{X_j = x\} \approx p_j(x) \equiv \frac{\lambda_j^x e^{-\lambda_j}}{x!} \quad [2]$$

To compute the average $r = \left\langle \frac{n}{n+m} \right\rangle$, we take the residual number of cells n to be distributed according to a probability distribution $\theta(n)$. The average r is computed in two different cases:

- (i) **ON-(-2)OFF passages:** The initial environment favors the ON frame hence most cells in the colony will be ON. In the next environment, only mutants with 2 bp deletions or large indels with length $l \equiv 1(\text{mod } 3)$ will survive. Therefore, the total number of surviving cells is

$$X_1 + X_4, \text{ and we obtain } r_1 \approx \sum_{n, x_1, x_4} \frac{n}{n + x_1 + x_4} \theta(n) p_1(x_1) p_2(x_4).$$

- (ii) **(-2)OFF->ON passages:** The initial environment favors the OFF frame and most cells in the colony are in the (-2)OFF frame. In the next environment, only mutants with 2 bp insertions or large indels with length $l \equiv 2(\text{mod } 3)$ will survive. Therefore, the total number of surviving

$$\text{cells is } X_2 + X_5, \text{ and we obtain } r_2 \approx \sum_{n, x_2, x_5} \frac{n}{n + x_2 + x_5} \theta(n) p_2(x_2) p_5(x_5).$$

Since the experiment alternates between these two types of passages, $r = (r_1 + r_2) / 2$.

The above result is evaluated numerically for Poisson-distributed n with different means, and different values of u , and plotted in Fig. S5A. In Fig. S5B, we compare results from simulations (see Materials and Methods, simulation variant A) with calculations across the full range of parameter values shown in Fig. S5A.

III: Bulk population model in the large population limit

Consider an exponentially growing population with two phenotypes adapted to each of two environments. Adapted individuals have growth rate f , and non-adaptive individuals have growth rate 0. At the end of environmental episode k , let R_k be the number of non-adapted individuals that existed at the beginning of the episode (i.e. the residual subpopulation), let M_k be the number of non-adapted novel mutants that occurred in this episode, and let A_k be the number of adapted individuals.

In episode $k + 1$, adapted individuals become non-adapted, stop dividing, and become the residual subpopulation at the end of the episode, that is

$$R_{k+1} = A_k \quad [3a]$$

The non-adapted individuals in episode k will be adapted in episode period $k+1$, start dividing, and generate new mutants, hence,

$$M_{k+1} = (R_k + M_k)\mu C \quad [3b]$$

$$A_{k+1} = (R_k + M_k)(1 - \mu)C \quad [3c]$$

where μ is the mutation rate of generating novel mutant, $C = 2^{\tau/\tau_d}$, τ is the environmental duration and $\tau_d = \log 2 / f$ is the doubling time for adaptive individuals. Note that $A_k = \frac{1 - \mu}{\mu} M_k$, and the dynamic of this system can be written as

$$\begin{pmatrix} R_{k+1} \\ M_{k+1} \end{pmatrix} = \begin{pmatrix} 0 & z \\ x & x \end{pmatrix} \begin{pmatrix} R_k \\ M_k \end{pmatrix} \quad [4],$$

with $z = \frac{1 - \mu}{\mu}$ and $x = \mu C$. The above recursion will approach steady-state growth in which a stable population composition is attained.

Defining $r_k = \frac{R_k}{R_k + M_k}$, r_k will approach a stationary value r , which is the *fraction of episodes in which the population used the ancestral allele mechanism to survive*. In the limit of large k , we have:

$$r = \frac{R_{k+1}}{R_{k+1} + M_{k+1}} = \frac{R_k}{R_k + M_k} \quad [5]$$

Substituting [4] into [5] and using $M_k = \frac{1-r}{r}R_k$, we obtain

$$za^2 = x(1+a) \quad [6]$$

where $a = \frac{1-r}{r}$. Solving the equation [6] yields

$$r = \left[1 + \frac{x + \sqrt{x^2 + 4zx}}{2z} \right]^{-1}. \quad [7]$$

For small mutation rates, $\varphi \approx 1 - r$. We compare exact results for φ shown in Fig. 4C,D vs. the approximate results using the above formula in Fig. S5C. As expected, the results based on r yield similar values in the regime $\mu \ll 1$.

Supporting Figure Captions

Figure S1: Schematic of experimental evolution & the *URA3* gene with a TR locus.

(A) Genetically-engineered *URA3* gene containing (AC)_n repeats after the ATG start codon. Arrows indicate primer pair used in PCR experiments to genotype TR sizes.

(B) Scheme for fluctuating selection. A common ancestral strain (*URA3* OFF) is used to found all lineages. A-lineages and B-lineages are passaged through fluctuating selection, using SC-Ura and SC+5FOA plates alternatively to perform selection and counter-selection. The first environment in A-lineages is selective, while the first environment in B-lineages is counter-selective. N-lineages using non-selective SC plates provide a control (neutral evolution).

Figure S2: Evolutionary trajectories of the A-lineages.

(A) Evolutionary trajectory of the A-lineages. The horizontal axis represents passages, and the vertical axis represents relative TR length (in bp) to the ancestral genotype. The horizontal gray lines correspond to in-frame TR lengths, and the vertical gray strips correspond to the selective environment.

(B) Lineage representation of the A-lineages. The color of each lineage corresponds to the color in (A). Gray, black, and white nodes represent non-selective, selective, and counter-selective environments. Nodes shown in red are the last node in each lineage, followed by extinction events.

Figure S3: Using fragment analysis results to infer TR sizes

(A) PCR triplicates for lineage A1, first selective node.

(B) PCR result of Lineage A1, first to fifth nodes.

Blue signals represent abundance of PCR product, and Red signals are the synthetic DNA marker with known lengths.

Figure S4: Growth rate bias between two OFF frames

(A) The coding region of the *URA3* (-2)OFF frame and (+2)OFF frame.

(B) Two strains with different OFF frames after 48 hrs incubation. Left upper sector: SC plate, Lineage A4, 5th node. Left lower sector: SC plate, Lineage A4, 3rd node. Right upper sector: SC +5FOA plate, Lineage A4, 5th node. Right lower sector: SC+5FOA plate, Lineage A4, 3rd node.

Figure S5: Calculation of frequency of ancestral allele mechanism (r) as a function of bottleneck size and mutation rate

(A) Calculation of r under the experimental bottleneck scheme. The red asterisk indicates the possible regime in the experiment.

(B) Comparison of calculated and simulated values of r .

(C) Analytical result obtained by using the bulk population model to compute $\phi \approx 1 - r$.

Supporting Tables & Table Captions

Table S1:

Strain	Mutation direction	TR length (bp)	Mutation rate; CI(95%) (10^{-4} per generation)
KV653 (replicate 1)	(-2)OFF-> ON	100	1.61; [1.32, 1.97]
KV653 (replicate 2)	(-2)OFF-> ON	100	1.28; [1.11, 1.49]
Lineage B1; 6 th node	(-2)OFF-> ON	118	2.95; [2.44, 3.57]
Lineage B1; 10 th node	(-2)OFF-> ON	112	3.06; [2.53, 3.71]
Lineage A4; 3 rd node	(-2)OFF-> ON	102	0.74; [0.66, 0.84]
Lineage A4; 5 th node	(+2)OFF-> ON	104	0.60; [0.49, 0.74]
KV653 (replicate 1)	ON-> OFF	100	0.491; [0.404, 0.540]
KV653 (replicate 2)	ON-> OFF	100	0.450; [0.388, 0.522]
Lineage B1; 7 th node	ON-> OFF	120	0.726; [0.637, 0.828]
Lineage B1; 11 th node	ON-> OFF	114	0.287; [0.245, 0.336]
KV948	ON-> OFF	15	0.00013; [0.00007, 0.00026]

Table S1: Mutation rates measured by fluctuation analysis

The mutation rate is measured by parallel culture and the mutant number distribution is fit to the Luria-Delbruck distribution.

Table S2:

Evolved Strain	<i>URA3</i> OFF frame type	Growth rate (1/hr) in SC medium	Growth rate (1/hr) in SC+5FOA medium
Lineage A3; 3 rd node	(-2)OFF	0.455± 0.036	0.407± 0.038
Lineage A3; 5 th node	(+2)OFF	0.448± 0.028	0.169± 0.060
Lineage A4; 3 rd node	(-2)OFF	0.494± 0.031	0.439± 0.010
Lineage A4; 5 th node	(+2)OFF	0.486± 0.046	0.199± 0.054

Table S2: Growth rates of (-2) and (+2) OFF frames in SC and SC+5FOA medium

The growth rates (mean ± S.D.) are measured by fitting the population growth curve in liquid cultures (three experimental replicates were performed for each value).

Table S3:

Strain	Mutation direction	Survival ratio (10^{-4})	Within TR length oscillation track?
Lineage B1; 6 th node	<i>URA3</i> (-2) OFF-> ON	2.00 ± 0.10	no
Lineage B1; 10 th node	<i>URA3</i> (-2) OFF-> ON	3.41 ± 0.19	yes
Lineage B4a; 4 th node	<i>URA3</i> (-2) OFF-> ON	1.00 ± 0.07	no
Lineage B4a; 8 th node	<i>URA3</i> (-2) OFF-> ON	0.83 ± 0.06	yes

Table S3: Survival frequencies of evolved population

The survival ratios (mean \pm S.D.) are determined by counting colony numbers in multiple plating on both selective and non-selective medium.

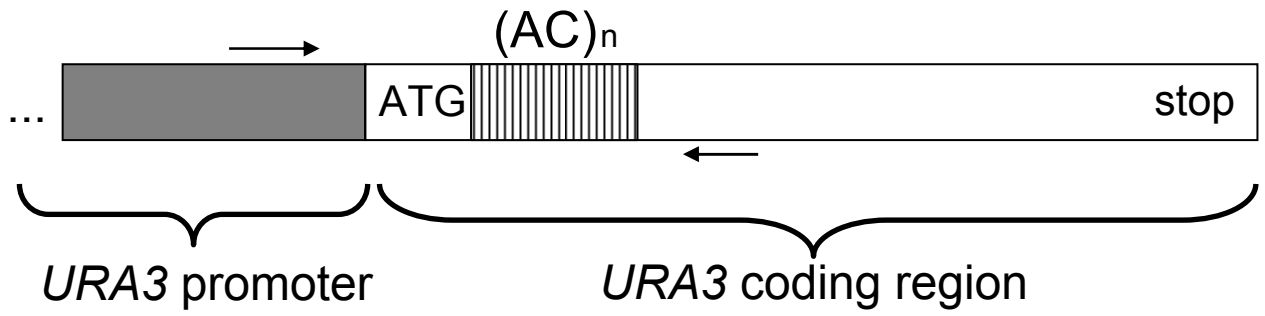
Table S4:

	parameter used in Fig 4A,B
Population size (N_{max})	2^{19}
Total mutation rate (u)	1.6×10^{-4}
Bottleneck (microcolony) size (n)	1~512
Large indel fraction (J)	0.4 for ON->OFF 0.1 for OFF->ON
Fitness in adaptive / non-adaptive environment	ON: 1.0 / 0.0 (-2)OFF: 0.0 / 1.0 (+2)OFF: 0.0 / 0.0

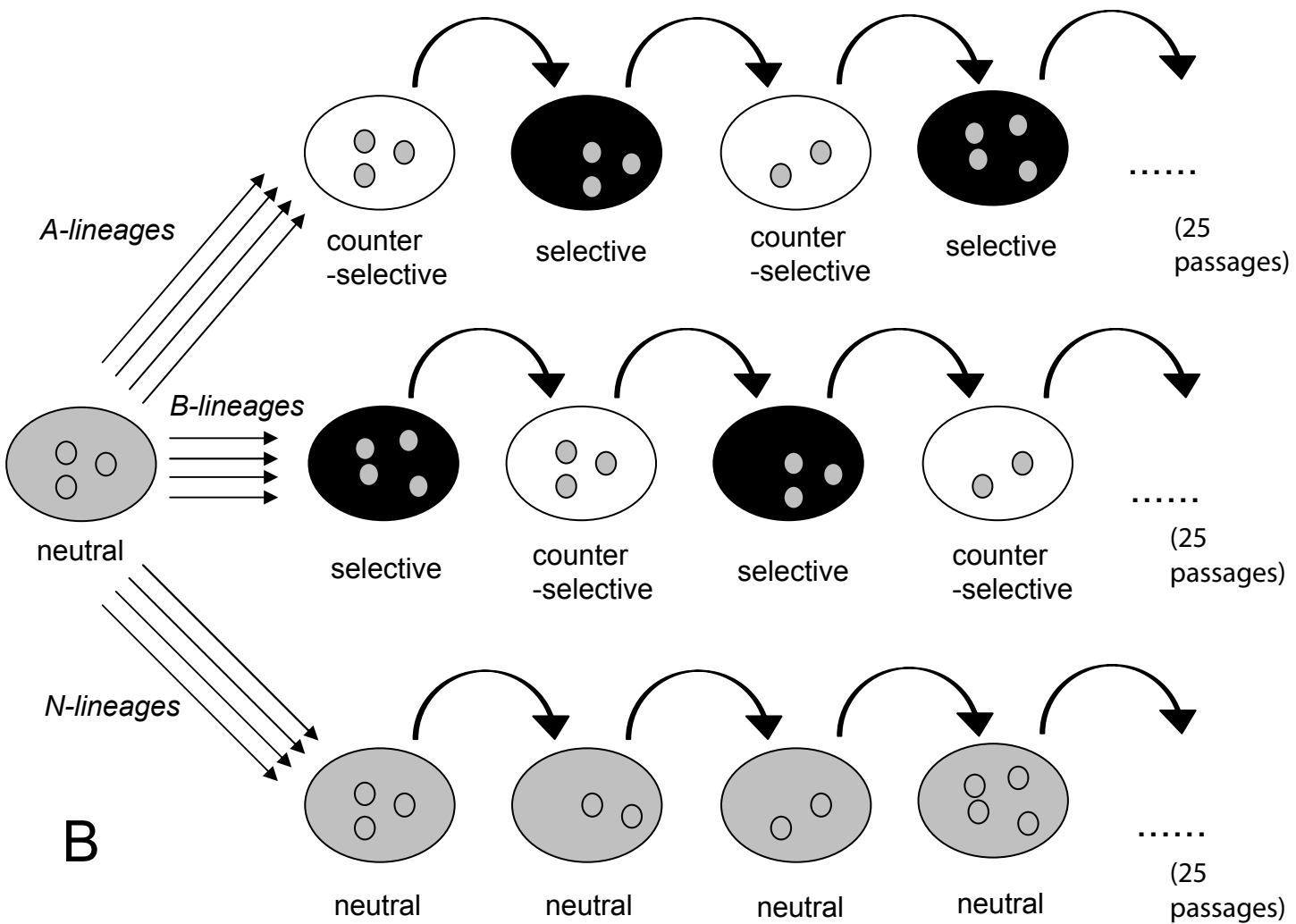
Table S4: Parameters used in mathematical model and simulation

References

- Delbruck, S. E. L. a. M. 1943. Mutations of Bacteria from Virus Sensitivity to Virus Resistance. *Genetics* 28:491.
- Gillespie, D. T. 2007. Stochastic simulation of chemical kinetics. *Annu Rev Phys Chem* 58:35-55.
- Hite, J. M., K. A. Eckert, and K. C. Cheng. 1996. Factors affecting fidelity of DNA synthesis during PCR amplification of d(CA)_n d(GT)_n microsatellite repeats. *Nucleic Acids Research* 24:2429-2434.
- Hoffman, C. S. and F. Winston. 1987. A ten-minute DNA preparation from yeast efficiently releases autonomous plasmids for transformation of *Escherichia coli*. *Gene* 57:267-272.
- Lang, G. I. and A. W. Murray. 2008. Estimating the per-base-pair mutation rate in the yeast *Saccharomyces cerevisiae*. *Genetics* 178:67-82.
- Legendre, M., N. Pochet, T. Pak, and K. J. Verstrepen. 2007. Sequence-based estimation of minisatellite and microsatellite repeat variability. *Genome Research* 17:1787-1796.
- Olejniczak, M. and W. J. Krzyzosiak. 2006. Genotyping of simple sequence repeats--factors implicated in shadow band generation revisited. *Electrophoresis* 27:3724-3734.
- Rosche, W. A. and P. L. Foster. 2000. Determining mutation rates in bacterial populations. *Methods* 20:4-17.
- Shinde, D., Y. Lai, F. Sun, and N. Arnheim. 2003. Taq DNA polymerase slippage mutation rates measured by PCR and quasi-likelihood analysis: (CA/GT)_n and (A/T)_n microsatellites. *Nucleic Acids Res* 31:974-980.
- Verstrepen, K. J., A. Jansen, F. Lewitter, and G. R. Fink. 2005. Intragenic tandem repeats generate functional variability. *Nat Genet* 37:986-990.
- W. T. Ma, G. V. S. a. S. S. 1992. Analysis of the Luria-Delbruck Distribution Using Discrete Convolution Powers. *Journal of Applied Probability* 29:255-267.



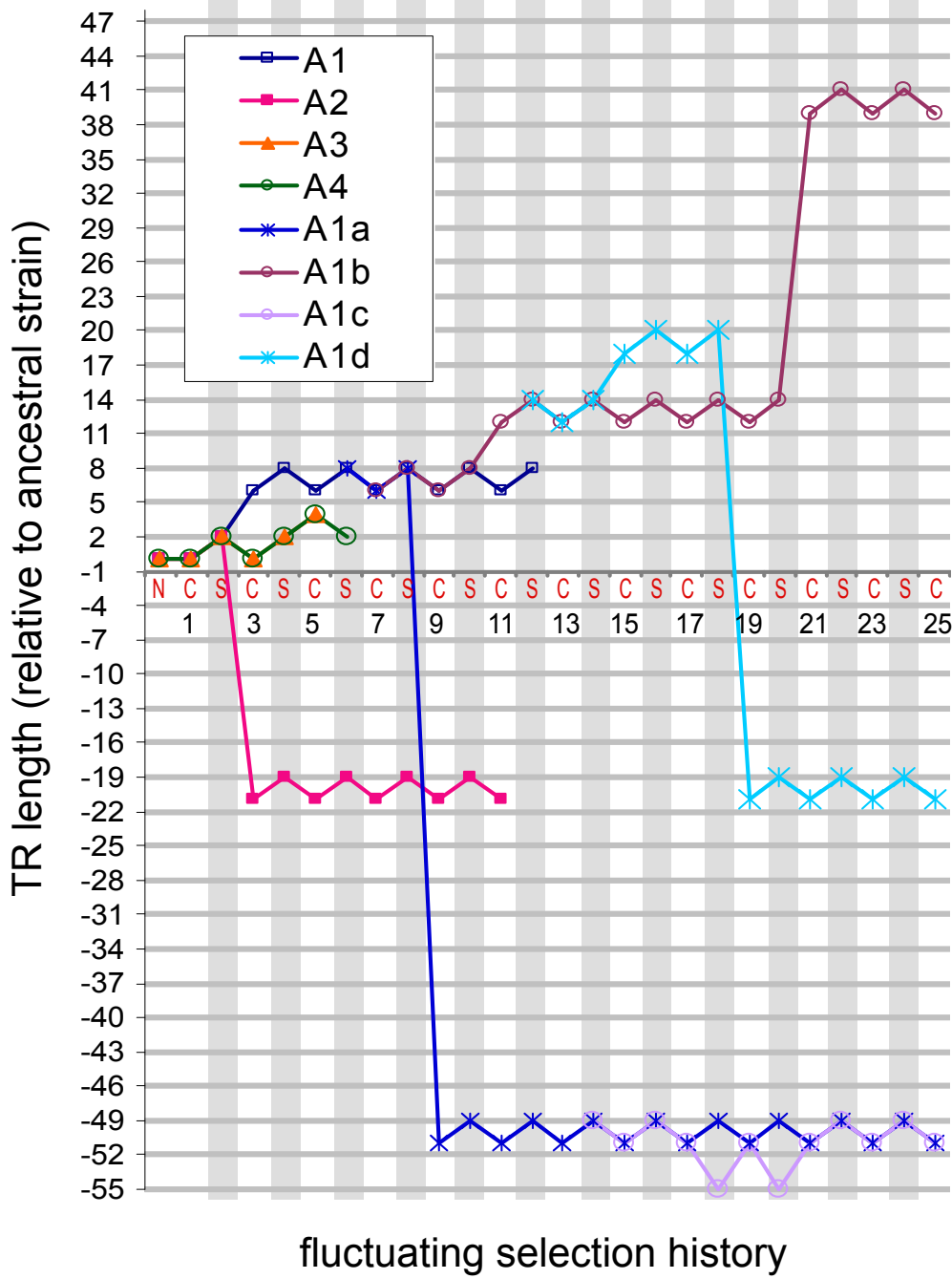
A



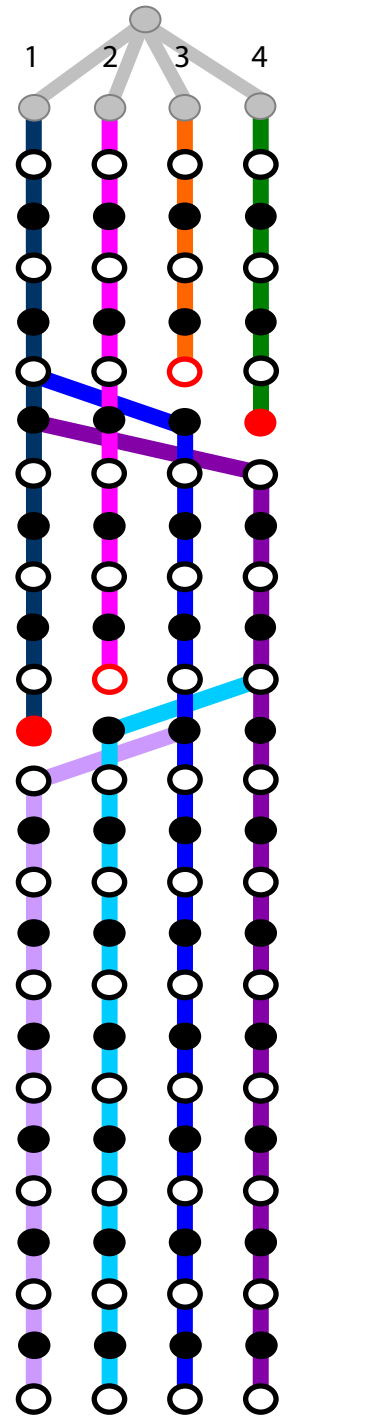
B

Figure S1

Figure S2



A



● non-selection
● selection
○ counter-selection

B

Figure S3

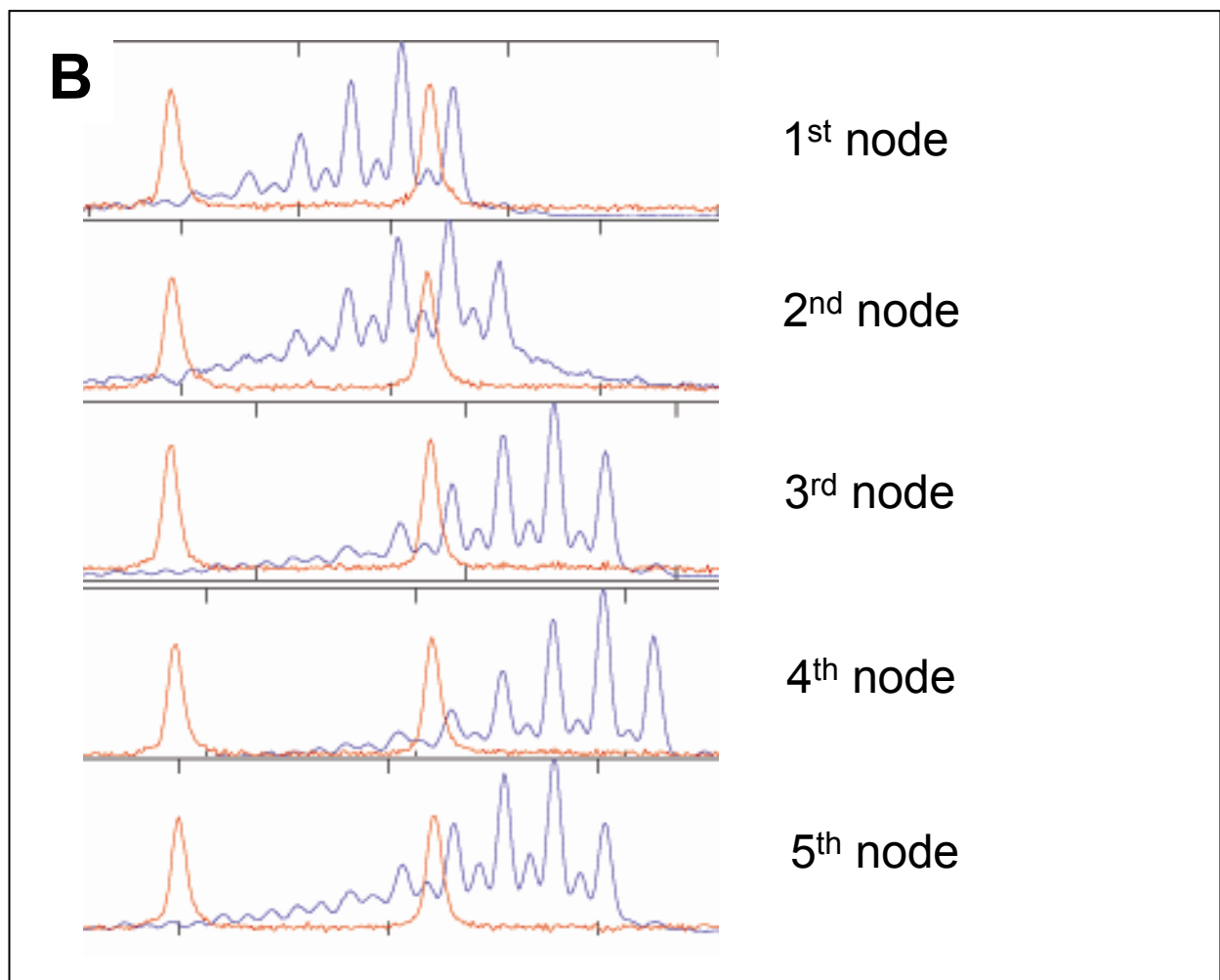
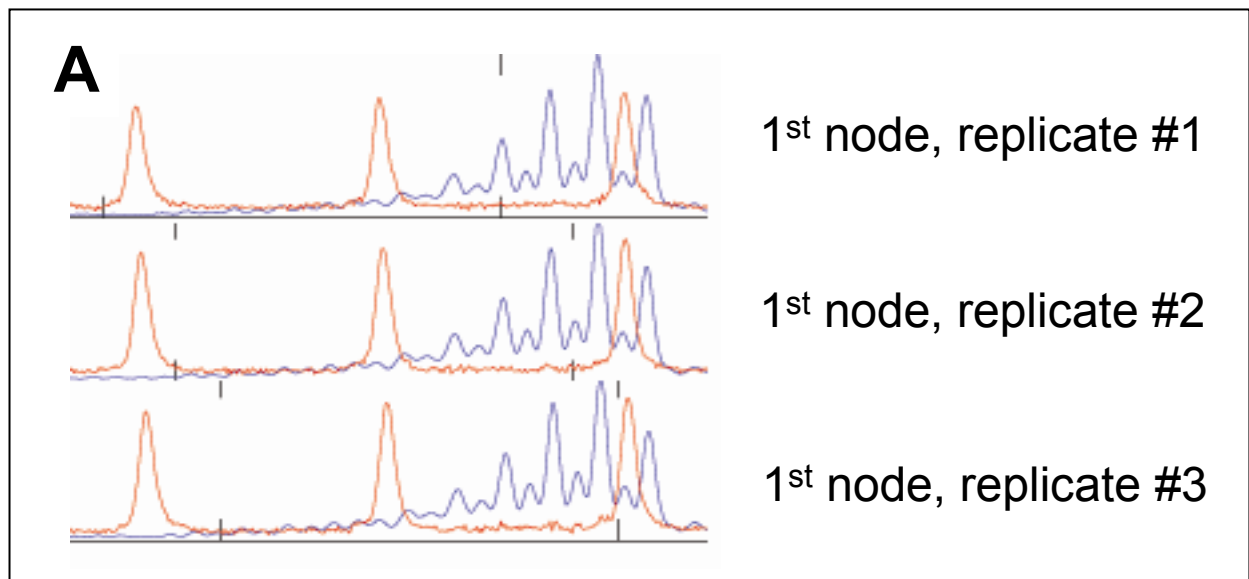


Figure S4

A *URA3* (+1)OFF frame

	Glu	Ser	Tyr	Ile	***	Gly	Thr	Cys	Cys	Tyr	Ser	Ser	***
ATGTCGAAAAG	CTACATATAA	GGAACGTGCT	GCTACTCATC	CTAGTCCTGT									

URA3 (+2)OFF frame

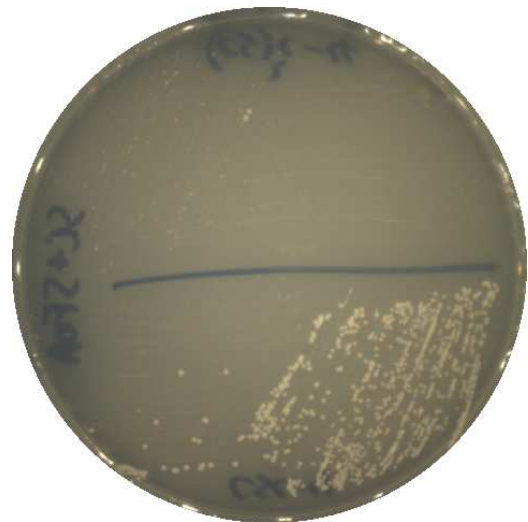
	Arg	Lys	Leu	His	Ile	Arg	Asn	Val	Leu	Leu	Leu	Ile	Leu	Val	Leu	Leu
ATGTCGAAAAG	CTACATATAA	GGAACGTGCT	GCTACTCATC	CTAGTCCTGT												
	Leu	Pro	Ser	Tyr	Leu	Ile	Ser	Cys	Thr	Lys	Ser	Lys	Gln	Thr	Cys	Val
TGCTGCCAAG	CTATTTAATA	TCATGCACGA	AAAGCAAACA	AACTTGTGTG												
	Leu	His	Trp	Met	Phe	Val	Pro	Pro	Arg	Asn	Tyr	Trp	Ser	***		
CTTCATTGGA	TGTTCGTACC	ACCAAGGAAT	TACTGGAGTT	AGTTGAAGCA												

B

Lineage B4, node #5
(+2)OFF frame

Lineage B4, node #5
(+2)OFF frame

SC plate



SC+5FOA plate

Lineage B4, node #3
(+1)OFF frame

Lineage B4, node #3
(+1)OFF frame

Figure S5

